

IV. 研究成果の刊行物・別刷

ガイドラインサポート
ハンドブック

大腸癌

大腸癌治療ガイドライン
2009年版

杉原健一 編

東京医科歯科大学大学院腫瘍外科学教授

医薬ジャーナル社

Q17 肝動注療法の有用性, その適応は?

A 肝動注療法の局所抗腫瘍効果は高く, 5-FU 以外に有効な薬剤がなかった時代では, 前治療なしの切除不能大腸癌肝転移に対する間歇的 5-FU 持続投与 (WHF 療法) の国内多施設での第 II 相試験の成績は奏効率 52%, 生存期間中央値 16.2 カ月であり¹⁾, 愛知県がんセンターでは奏効率 78%, 生存期間中央値 25.8 カ月であった²⁾。このため, かつては汎用されていたが, 欧米での全身化学療法との比較試験で生存期間における優位性が証明されなかったことやその後の FOLFOX, FOLFIRI 療法といった標準療法の確立に伴い日本でも一次治療として肝動注が行われる機会は著しく減少している。

この状況下での肝転移に対する肝動注の適応, 位置づけを明確にすることは困難であるが, その高い局所制御効果とともに副作用が軽微であることも勘案して戦略を考慮すべきである。全身状態不良や肝機能低下などの理由により標準化学療法の施行が躊躇される症例, 末梢神経毒性, 骨髄抑制, 消化器毒性などの副作用により標準療法が継続困難となった症例, 標準療法で効果の得られない, あるいは標準療法による治療効果が得られなくなった段階の肝転移が予後に大きく影響すると考えられる症例では肝動注は許容される。

ただし, 標準治療後の 5-FU のみによる肝動注療法の成績は前治療なしの場合に比べ低いと一般に認識されており, イリノテカンやオキサリプラチンなどとの併用(動注または全身投与)が試みられることもあるが, その効果は現時点では不明である。

また, 肝動注の施行においては, 動注用カテーテル・リザーバーの設置が必須であり, 適切な薬剤分布が得られるようにカテーテルを留置する技術も要求される³⁾。

(稲葉吉隆)

(文 献)

- 1) 熊田 卓, 荒井保明, 伊藤和樹ほか: 大腸癌肝転移に対する大量 5-FU 週 1 回 5 時間持続動注療法—多施設共同研究—. 日本癌治療学会雑誌 28 : 1449, 1993
- 2) Arai Y, Inaba Y, Takeuchi Y, et al : Intermittent hepatic arterial infusion of high-dose 5FU on a weekly schedule for liver metastases from colorectal cancer. Cancer Chemother Pharmacol 40 : 526-530, 1997
- 3) Seki H, Kimura M, Yoshimura N, et al : Hepatic arterial infusion chemotherapy using percutaneous catheter placement with an implantable port : assessment of factors affecting patency of the hepatic artery. Clin Radiol 54 : 221-227, 1999

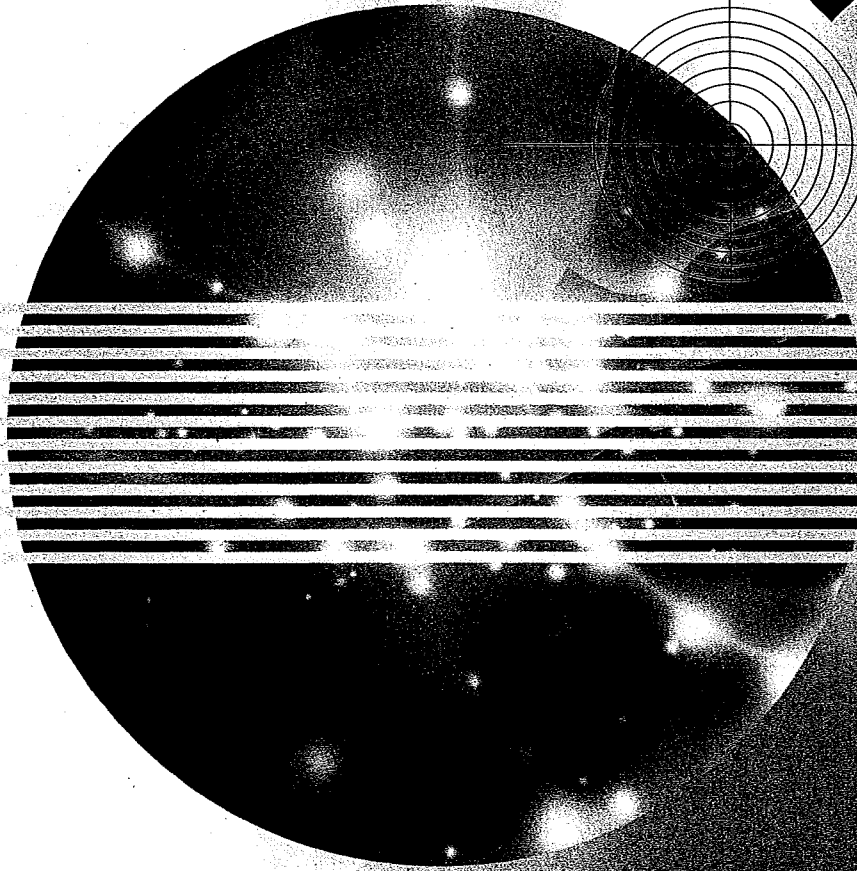
新臨床腫瘍学

がん薬物療法専門医のために

日本臨床腫瘍学会

[編集]

改訂
第2版



南江堂

③ BCR/ABL 阻害薬, c-KIT 阻害薬	島 清彦	344
④ mTOR 阻害薬	田村研治	347
⑤ その他のシグナル伝達系阻害薬	土井俊彦	350
2) 血管新生阻害薬・多標的阻害薬	向原 徹	355
3) 抗体薬		361
① 総論	飛内賢正	361
② 細胞表面抗原に対する抗体薬	飛内賢正	364
③ 上皮成長因子受容体に対する抗体薬	大津 敦	370
④ trastuzumab	勝俣範之	374
⑤ bevacizumab	清田尚臣	378
4) プロテアソーム阻害薬	堀田知光	383
5) エピジェネティクス標的薬	富田章裕	386
6) その他の分子標的治療薬	藤阪保仁	391
⑩ 新しい治療戦略		395
1) 遺伝子治療, アンチセンス, RNAi	瀧本理修	395
2) がん免疫療法	平家勇司	399

III. Practice of Oncology

403

⑩ 抗がん薬の投与方法		404
1) ポートの留置・管理	稲葉吉隆	404
2) 髄腔内ならびに Ommaya reservoir を介した薬物療法	田村和夫	408
3) 腹腔内薬物療法	藤原恵一	412
⑪ 頭頸部がん	田原 信	416
⑫ 肺がん		427
1) 小細胞がん	大江裕一郎	427
2) 非小細胞がん	武田晃司・多田弘人	434
⑬ 中皮腫	中野孝司	447
⑭ 縦隔腫瘍	関根郁夫	452
⑮ 乳がん	清水千佳子	457
⑯ 食道がん	加藤 健	471
⑰ 胃がん	山口研成	483
⑱ 結腸・直腸がん, 肛門がん	吉野孝之	495
⑲ 消化管間質腫瘍	小松嘉人	510
⑳ 原発性肝がん	古瀬純司	518
① 肝細胞がん		519
② 肝内胆管がん		525
㉑ 膵がん	朴 成和	528
㉒ 胆道系がん	奥坂拓志	535
㉓ 腎細胞がん	富田善彦	542

1 ポートの留置・管理

1. 皮下埋め込み型ポート

必要時に体外から皮膚を介して穿刺し、薬剤などを注入あるいは体腔液を回収するための器具をポートまたはリザーバーと呼び、目的部位(血管内や腹腔内など)に挿入されたカテーテルと接続して皮下に埋め込み使用される。

2. 中心静脈ポート

中心静脈ポート設置の適応は、中心静脈栄養と悪性腫瘍患者における抗がん薬や鎮痛薬などの静脈内持続注入とされている。

中心静脈カテーテルを完全皮下埋め込み型にすることで、中心静脈への薬剤投与が安全で簡便なものとなり、中心静脈カテーテルの留置に伴う患者のQOLの低下を防ぐことができる。中心静脈ポートを利用することにより薬剤投与は計画的・継続的に施行可能となり、持続投与や頻回投与を含む外来薬物療法や在宅療養における中心静脈栄養が容易となる。とくに大腸がんに対する薬物療法において、FOLFOX療法やFOLFIRI療法が標準療法として導入され、これらには5-FUの持続静注が含まれるため、外来ベースで運用するには中心静脈ポートと携帯用注入ポンプの使用が必須となる。

ただし、カテーテル・ポートシステムは異物を体内に留置することとなるため、感染、血栓形成、皮膚障害、薬液漏出、器具の破損などが生じるこ

とがあり、不適切な使用や対応が重大な問題に発展し得るものであることに留意すべきである。重篤な出血傾向・血液凝固異常、刺入血管閉塞などは設置そのものが禁忌となる。

3. 器具の選択

ポートの基本構造は留置カテーテルとの接続部(コネクター)、内室(チャンバー)、天井隔壁(セプタム)により構成され、シリコン製のセプタムを経皮的に穿刺することでチャンバーを介してカテーテルと通じることとなる。ポートの大きさ・形状は、留置(埋設)部位、体型、皮下脂肪の状況などにより、ポートの安定性と穿刺しやすさも考慮して選択される。

ポートと接続して中心静脈内に留置されるカテーテルには、カテーテル先端がそのまま開口しているタイプとスリット状の特殊弁となって開口するタイプ[グローションカテーテル(先端盲端・側面スリット)：バード/メディコン、オルカカテーテル(先端スリット)：パイオラックス/住友ベークライト]があり、使用カテーテルがどのタイプなのか周知しておく必要がある。先端開口タイプでは通常の中静脈カテーテルと同様に、薬液注入終了時には、血液の逆流による閉塞を防止するために、ヘパリン加生理食塩水または生理食塩水を充填する必要がある。特殊弁となっているタイプは薬液注入時のみ開口し、血液逆流はしないようになっているので、あえてヘパリン加生理食塩水を充填する必要はないとされている。

4. 中心静脈ポート設置（埋め込み）位置の選択

通常、中心静脈カテーテルを挿入できる部位であればポートの設置はおおむね可能であるため、カテーテル刺入血管として腋窩～鎖骨下静脈が選択されることが多いが、内頸静脈、前腕静脈、上腕静脈、大腿静脈なども用いられる。ただし、ポートが接続されて皮下に埋め込まれるため、解剖学的にポートの安定性がよく、患者の動きや生活に支障をきたさない部位が考慮されるべきである。自己管理の面から、右利きの患者の場合は、左鎖骨下や左上肢にポートを設置することを推奨している施設もある。

鎖骨下にポートを留置する場合は、鎖骨下静脈のピンチオフエリアと呼ばれる第1肋骨と鎖骨が交差する部位を介しての穿刺は避け、それより外側の腋窩静脈領域での穿刺が推奨される。カテーテルピンチオフとは、鎖骨下静脈に刺入されたカテーテルが第1肋骨と鎖骨に挟み込まれてカテーテルの閉塞や損傷をきたす現象で、鎖骨下静脈から挿入されたカテーテルに特有の合併症である。

5. 中心静脈ポート設置方法

カテーテルの挿入方法は、基本的には通常、中心静脈カテーテルの挿入法と同様であるが、従来の解剖学的指標をもとに画像を用いずに穿刺する方法やX線透視のみで穿刺する方法よりは、造影透視や超音波を用いて静脈を確認しながら穿刺する方法が推奨される。静脈穿刺後は、ガイドワイヤを用いて透視下操作により確実に目的部位までカテーテルを挿入する。皮下トンネルを通したカテーテルとポートを接続して、適切な位置に作成した皮下ポケットに埋設する。はじめに皮下ポケットを作成して、その皮膚切開部から静脈を穿刺して皮下トンネルを通さない方法もある。

以下に造影透視を用いた設置方法を紹介する。造影透視が可能な血管造影室またはX線テレビ室にて、肘静脈より造影剤を数mL注入し、腋窩静

脈から鎖骨下静脈の走行と開存性（まれではあるが、腕頭静脈で閉塞している症例が経験される）を透視下に確認し、およその穿刺位置や皮膚切開部位を決定する。消毒、局所麻酔後、ポートの大きさに合わせて皮膚切開し、皮下ポケットを作成する。再度、肘静脈より造影剤を約10mL注入し、腋窩静脈から鎖骨下静脈の走行を透視下に確認しながら、皮切部より穿刺針を進めて静脈を穿刺する。第1肋骨の直上の腋窩静脈内側部を目標とする。静脈血の逆流を確認しガイドワイヤを上大静脈まで進め、カテーテルを上大静脈まで挿入する。留置用キットにシース付きダイレーターがある場合は利用する。カテーテル先端位置を調節し、カテーテルの手元側を皮下ポケットの位置に合わせて切断しポートと接続し、ノンコアリング針でポートを穿刺して生理食塩水でフラッシュして、カテーテル閉塞や損傷がないことを確認してから皮下に埋設する。

カテーテルの取り扱いやカテーテルとポートの接続法は個々の製品により異なるので、使用説明書により注意点を熟知しておく必要がある。

6. 外来薬物療法での使用方法

大腸がんに対するFOLFOX療法やFOLFIRI療法などの5-FU持続静注を含んだ薬物療法の実際について紹介する。外来担当医による当日の治療実施可能の判断のもとに薬物療法が開始される。ポート部皮膚面をアルコール綿で消毒し、生理食塩水または注射用蒸留水入りのシリンジと接続した24Gまたは22Gのノンコアリング針でポートを穿刺する。ポート中央のセプタム部をポート底に当たるまでゆっくりと穿刺し、生理食塩水または注射用蒸留水でポートからカテーテル内腔をフラッシュする。これによりポートシステムに異常がないことを確認し、薬液注入を開始する。ポートを穿刺する感覚、フラッシュする感覚を経験によりつかんでおくことが重要である。異常を感知した場合は、ポート設置医に連絡し造影などにより異常の有無を確認する。

5-FU持続静注はディスプレイの携帯用注入

Ⅲ章 Practice of Oncology

ポンプ(インフューザー)を用いて行う。規定用量の5-FUを生理食塩水または注射用蒸留水により総量を調整して使用する。ディスプレイインフューザーは温度、粘度、濃度により注入速度が異なってくるので、各製品の調整表に基づき総量を調整し、体温センサー(流量制御部)付きの製品では確実に皮膚面に貼り付ける。接続管の屈曲には注意して固定してクレンメを開放する。

薬剤投与終了時は、カテーテルの種類により対応が異なる。通常の先端開口型カテーテルの場合は、十分量のヘパリン溶液などでロックする。逆流防止機能を備えたカテーテルの場合には、ヘパリンロックは必要ではないが、生理食塩水または注射用蒸留水でのフラッシュがすすめられる。ただし、インフューザーを使用して5-FUの持続静注を行い、在宅で自己抜針する場合は定期使用となることもあり、抜針時のフラッシュは必ずしも必要としない。

7. 中心静脈ポートの管理

a) ポート穿刺に使用するべき針

穿刺にはシリコンセプタムを削り取らないように専用針(ノンコアリング針)を使用する。ノンコアリング針の使用により、通常型ポートは22G針で2,000回以上の穿刺に耐えられることとなっている。一般に、針径が太くなる(18Gや20G)と耐用回数は落ち、細くなる(24G)と多くなるとされている。また、セプタムの中心部分を集中的に穿刺した場合には穿刺耐用回数はより少ないものとなり注意を要する。

針の長さは5/8インチ長が汎用されるが、ポート設置部の皮下脂肪の厚さとポートサイズにより、長め(3/4インチ長)または短め(1/2インチ長)の針を選択し、適切な穿刺(針の先端がポートの底面まで届き、皮膚面から固定翼部が離れ過ぎない)になるように調節する。最近では、誤穿刺防止のため抜針時に針の先端部を覆うようになるような安全機構付きのポート専用穿刺針も市販されている。

b) 穿刺時の消毒

海外のガイドラインでは、2% chlorhexidine がカテーテル関連感染予防のため推奨されているが、70%アルコール(アルコール綿、酒精綿)、10% povidone-iodine でも可としている。アルコール綿は作用時間が短いものの殺菌作用に優れており、povidone-iodine はアルコールよりも作用時間が長いものの殺菌作用にやや劣るとされている。消毒薬の選択は施設基準に沿って行われることがほとんどであるが、過敏症には十分留意する。一般には通常の静脈注射時と同様に、穿刺部からその周囲の皮膚面をアルコール綿で消毒することで十分であり、アルコール過敏者やポート感染やカテーテル感染の既往者などでは povidone-iodine が用いられる。povidone-iodine 使用時は乾燥してから穿刺する。

8. 合併症とその対策

a) 設置時の合併症

通常の中静脈カテーテル挿入と同様に気胸、出血、動脈穿刺、疼痛などがあげられる。局所麻酔薬などの使用薬剤過敏には要注意である。

b) カテーテル機能不全

カテーテルピンチオフなどによるカテーテル損傷、フィブリンシースや血栓、捻れ、屈曲などによるカテーテル閉塞によって生じる。X線透視またはX線写真によりカテーテルの留置状況を確認し、必要に応じてポートからの造影を行い原因究明の上、原則としてシステムを抜去し再留置する。血栓閉塞が疑われる場合は、生理食塩水の圧入や血栓溶解薬の注入を試みることもあるが、強く圧入するとカテーテル損傷やカテーテル接続部離脱を招くことがあり注意を要する。

c) 血栓性静脈炎、静脈血栓症

カテーテル留置血管での血栓形成や静脈炎を生じた場合には、抗凝固療法、消炎薬や抗生物質の使用を検討する。症状によりシステムを抜去する。上大静脈症候群や肺動脈血栓・塞栓症を生じるこ

ともあり得るので、十分な状態観察を要する。

d) 薬剤の皮下漏出

穿刺針が抜けてきて浅くなった場合(抜浅), カテーテル損傷, カテーテル接続部離脱, ポートセプタム破損により発生する。システム損傷に起因する場合は抜去再留置する。穿刺針抜浅による場合は穿刺法やテープ固定法を再確認する。抗がん薬の漏出時は早急にステロイド局注などの処置を行い, 状況により皮膚科専門医にコンサルトする。

e) 皮膚障害

ポート被覆部で皮膚発赤・びらん・潰瘍やポート露出を生じることがある。発赤・びらん程度では一定期間不使用, 軟膏処置で対応する。潰瘍形成やポート露出に至る場合や感染を伴う場合はシステム抜去を要する。皮膚形成が必要となる場合もある。

f) 感染

カテーテル感染, ポート周囲感染が生じ得る。カテーテル感染が疑われる場合(カテーテル吸引培養でも陰性のことも多い)は抗生物質の投与やシステム充填を試みるが, 結局システム抜去が必要となることが多い。ポート周囲感染ではただちにシステムを抜去する。

9. 動注ポートの注意点(中心静脈ポートと異なる点)

留置された状態は見た目がほとんど同じため, 留置情報の共有と患者への説明は必須である。両者が留置されている場合(ダブルポート)にはとく

に注意を要する。動脈圧がかかるため動注ポートの使用には血液逆流に注意を払う。薬液投与は自然滴下できないため陽圧注入が必要である。使用終了時には, ヘパリン原液またはヘパリン加生理食塩水を陽圧注入下に抜針する。

また, カテーテルは選択的に目的臓器の動脈まで挿入されており, 抗がん薬が投与される領域を把握しておく必要がある。高濃度の抗がん薬が局所に注入されることに伴い生じ得る合併症についての理解が要求される。動注により何らかの症状が生じる場合や動注関連が疑われる症状が生じている場合には, まずは薬剤投与を中止して, 対処可能なものには早急に対応する。

※参考文献

- 1) Biffi R, De Braud F, Orsi F et al : A randomized, prospective trial of central venous ports connected to standard open-ended or Groshong catheters in adult oncology patients. *Cancer* 92 : 1204-1212, 2001
- 2) Biffi R, Orsi F, Pozzi S et al : Best choice of central venous insertion site for the prevention of catheter-related complications in adult patients who need cancer therapy : a randomized trial. *Ann Oncol* 2009 [Epub ahead of print]
- 3) Vescia S, Baumgartner AK, Jacobs VR et al : Management of venous port systems in oncology: a review of current evidence. *Ann Oncol* 19 : 9-15, 2008
- 4) Mansfield PF, Hohn DC, Fornage BD et al : Complications and failures of subclavian-vein catheterization. *N Engl J Med* 331 : 1735-1738, 1994
- 5) Inaba Y, Yamaura H, Sato Y et al : Central venous access port-related complications in outpatient chemotherapy for colorectal cancer. *Jpn J Clin Oncol* 37 : 951-954, 2007

□ CASE REPORT □

Jejunogastric Intussusception: Life-Threatening Complication Occuring 55 Years after Gastrojejunostomy

Hiroyuki Tokue¹, Yoshito Tsushima², Yasuaki Arai¹ and Keigo Endo²

Abstract

An 80-year-old man presented with acute abdominal pain and hematemesis. He had a history of gastrojejunostomy 55 years previously. Ultrasonography (US) showed intragastric tubular images with peristalsis. Enhanced computed tomography (CT) demonstrated a dilated stomach with an intragastric filling by bowel loops suggestive of jejunogastric intussusception (JGI). Reduction of the JGI was immediately performed without resection of the intussuscepted intestine, and the patient was well postoperatively.

JGI is a rare life-threatening complication after gastric surgery. This complication may occur even 55 years after gastric surgery, and preoperative diagnosis is possible by US and CT findings.

Key words: jejunogastric intussusception, invagination, gastric surgery, computed tomography, ultrasonography

(*Inter Med* 48: 1657-1660, 2009)

(DOI: 10.2169/internalmedicine.48.2115)

Introduction

Jejunogastric intussusception (JGI) is a rare life-threatening complication of gastrectomy or gastrojejunostomy. It usually occurs with abdominal pain, nausea, vomiting, and hematemesis. Diagnosis of this condition has been reported to be difficult in most of the cases, although a history of gastric surgery can help in making a diagnosis. An early diagnosis and urgent surgical intervention are essential. We present a case of the characteristic US and CT findings of this entity.

Case Report

An 80-year-old man presented with acute abdominal pain and hematemesis. He had undergone gastrojejunostomy (Billroth II reconstruction) for a bleeding duodenal ulcer 55 years previously. Physical examinations disclosed epigastric tenderness and a soft non-distended abdomen. His vital signs were normal and blood counts and laboratory examinations were unremarkable. Ultrasonography (US) showed intragastric tubular images with peristalsis (Fig. 1), and en-

hanced computed tomography (CT) demonstrated a dilated stomach with an intragastric filling by bowel loops (Fig. 2). We suspected JGI based on imaging findings, and endoscopy confirmed it with petechial hemorrhage (Fig. 3). Emergent surgery revealed a severely dilated stomach stump and a 40 cm-long efferent intestinal loop which had intussuscepted in a retrograde direction into the remnant gastric lumen, passing over the Braun's anastomosis (Fig. 4). His operative findings were Billroth II retrocolic loop gastrojejunostomy. The efferent loop was edematous with serosal petechiae but absolutely viable. No abnormalities such as a tumor, ulcer, diverticulum, or stenosis were identified that could have acted as a point for the intussusception. Reduction of the JGI was performed by Hutchinson's procedure without resection of the intussuscepted intestine. He was well postoperatively and discharged nine days after operation. On follow-up, his postoperative course was uneventful.

Discussion

JGI was first described by Bozzi (1) in a patient after gastrojejunostomy, and it was also reported in patients after Billroth I reconstruction, Billroth II reconstruction, total gas-

¹Division of Diagnostic Radiology, National Cancer Center Hospital, Tokyo and ²Department of Diagnostic and Interventional Radiology, Gunma University Hospital, Maebashi

Received for publication February 3, 2009; Accepted for publication May 27, 2009

Correspondence to Dr. Hiroyuki Tokue, tokue@s2.dion.ne.jp

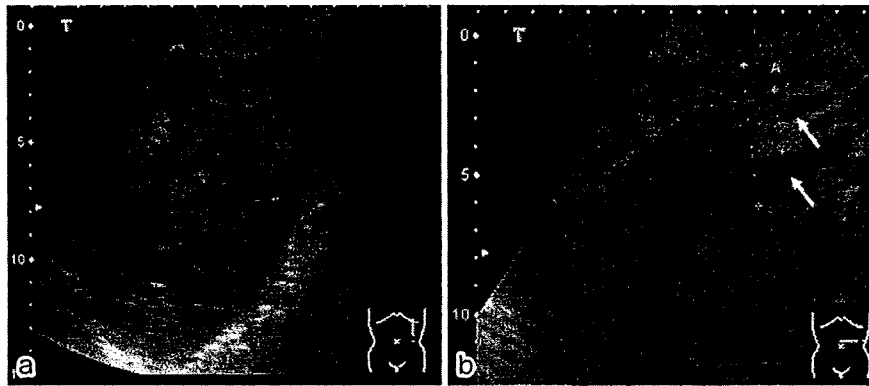


Figure 1. A 80-year-old man presented with abdominal pain and hematemesis. (a) Sagittal US demonstrated intragastric tubular images with peristalsis. (b) Transverse US revealed a sandwich-like appearance (arrows) of the alternating loops of bowel with a loop-within-loop appearance.

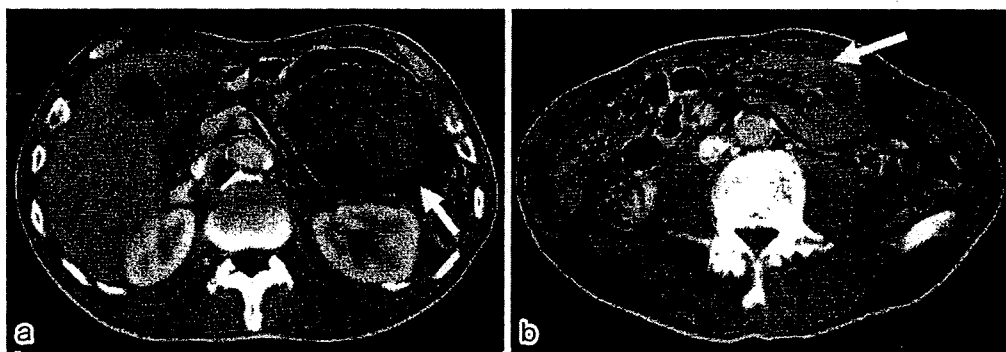


Figure 2. (a) Enhanced CT showed a distended stomach with an intragastric filling by bowel loops (arrow). (b) Mesenteric fat and vessels were followed into the intussusception with central area of fat density and vessels (arrow).

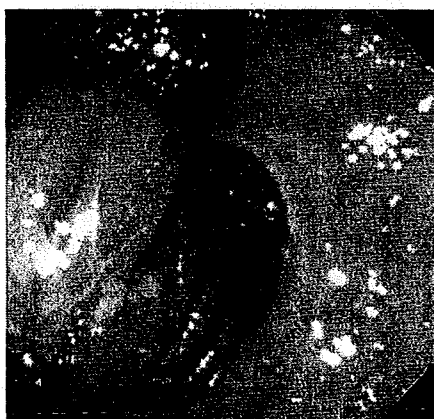


Figure 3. Gastric endoscopy showed a lobulated congestive mass which was consistent with jejuno-gastric intussusception.

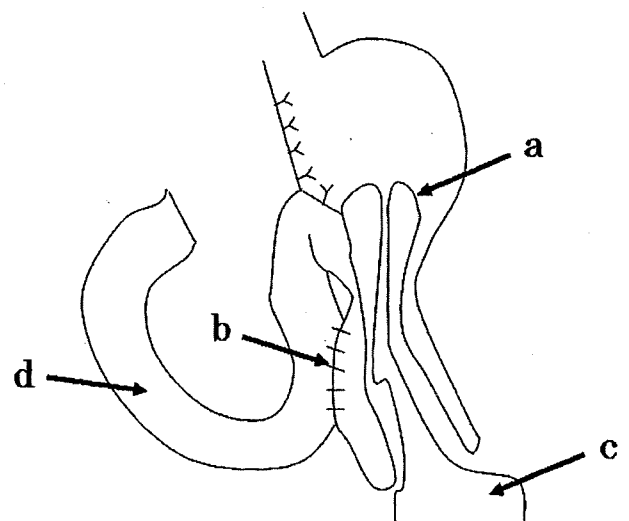


Figure 4. The operative findings: (a) retrograde jejuno-gastric intussusception (b) Braun's anastomosis (c) dilated efferent loop (d) afferent loop.

trectomy, Roux-en-Y gastric bypass, and a pancreaticojejunostomy (2-4). The incidence of JGI has been estimated to be three in 2000 gastrojejunostomies (0.15%) (5). Although there have been many case reports about JGI in the surgical literature (6-8), it has been rarely reported in the field of internal medicine. A possible race difference has not been investigated, however, the incidence may be extremely low in

Asia; there have only been a few case reports from Asian countries (9, 10). Physician should be aware of the US and CT findings of this life-threatening complication after gastric

surgery.

The etiology of JGI is unclear. Two major theories are functional and mechanical. The most widely accepted functional theory is the disordered motility with functional hyperperistalsis triggered by spasm or hyperacidity (11). Mechanical factors include adhesions, a long mesentery, gastric derangements, and a sudden increase in abdominal pressure (12). An acute and a chronic form of JGI have been clinically recognized (5). Incarceration and strangulation of the intussuscepted loop generally occur in the acute form. On the other hand, spontaneous reduction is typical in the chronic type. Thus, the acute form like the present case is characterized by acute severe colicky epigastric pain, vomiting and, subsequently, hematemesis. JGI is classified into three anatomic types according to the invaginated loop (13), type I: afferent loop invagination, type II: efferent loop invagination, type III: the intussusception of both. A type II invagination is observed in 80% of cases (3) and our case was classified type II.

Shiffman and Rappaport (6) emphasized that loose mucosa at the anatomic site may prolapse into the gastric pouch during normal peristalsis. This could explain the less common afferent loop intussusception. Karlstrom and Kelly (14) suggested that ectopic pacemakers present in the Roux limb after vagotomy and Roux gastrectomy drive the limb in the reverse direction and slow emptying of liquids after operation. The defect can be corrected by pacing the Roux limb in the forward direction. In the present case, the efferent loop was found intussuscepted in a retrograde way into the gastric lumen. These reports may explain the cause of the present case. JGI has occurred between five days to 35 years after surgery (5). The present case occurred 55 years after surgery and as far as we know this case is the longest period from operation in past reports.

US is the method of first choice because it can be performed at bedside without ionizing radiation and is cost-effective. CT allows the differentiation of the distinct stages of the disease and the views given by CT are often more easily accepted by the surgeons. It is important to understand the typical imaging findings of JGI. In most cases, US shows intragastric tubular images with peristalsis and CT shows a dilated stomach with intragastric filling by bowel loops (3, 15). Most reported cases of JGI were diagnosed at surgery (16), but we suspected that the typical findings enable us to make preoperative diagnosis. Although spontaneous reduction was reported, in most cases surgical management should be performed as soon as possible to avoid the additional risk of severe complications. Surgical options include reduction, resection of the compromised bowel, revision of the anastomosis, and the takedown of the anastomosis, depending on the conditions found during the operation (3). When there is ischemic change of the invaginated loop, resection is the only treatment option. In the acute setting, the morbidity and mortality figures vary considerably, with mortality rates rising significantly from 10 to 50% with 48 hours delay in surgical correction (17). The fixation of the jejunum to the adjacent tissue, mesocolon, colon, or stomach may obviate the recurrence (18).

Conclusion

JGI is a rare life-threatening complication of gastric surgery which is often diagnosed at surgery. There is a wide variation in the lapse time between the gastric surgery and the occurrence of JGI. This complication may occur even 55 years after gastric surgery; preoperative diagnosis is possible by US and CT findings. We should be aware of these imaging findings to avoid mortality.

References

1. Bozzi E. Annotation. *Bull Acad Med* 122: 3-4, 1914.
2. Lundberg S. Retrograde dunndarminvagination nach gastroenterostomie. *Acta Chir Scand* 54: 423-433, 1922.
3. Archimandritis AJ, Hatzopoulos N, Hatzinikolaou P, et al. Jejunogastric intussusception presented with hematemesis: a case presentation and review of the literature. *Gastroenterol* 1: 1, 2001.
4. Goverman J, Greenwald M, Gellman L, Gadaleta D. Antiperistaltic (retrograde) intussusception after Roux-en-Y gastric bypass. *J Am Coll Surg* 199: 988-989, 2004.
5. Marx WJ. Reduction of jejuno gastric intussusception during upper gastrointestinal examination. *Am J Roentgenol* 131: 334-335, 1978.
6. Shiffman M, Rappaport I. Intussusception following gastric resection. *Am Surg* 32: 715-724, 1966.
7. Salem MH, Coffman SE, Postlethwait RW. Retrograde intussusception at the gastrojejunal stoma. *Ann Surg* 150: 864-871, 1959.
8. Wheatley MJ. Jejunogastric intussusception diagnosis and management. *J Clin Gastroenterol* 11: 452-454, 1989.
9. Hashimoto Y, Akagi S, Sakashita Y, et al. Usefulness of computed tomography as a preoperative diagnostic modality in a case with acute jejuno gastric intussusception. *J Gastrointest Surg* 11: 1078-1080, 2007.
10. Su MY, Lien JM, Lee CS, Lin DY, Tsai MH. Acute jejuno gastric intussusception: report of five cases. *Chang Gung Med J* 24: 50-56, 2001.
11. Robertson DS, Weder C. Acute jejuno gastric intussusception. *Can J Surg* 1: 210-214, 1968.
12. Bundrick TJ, Turner MA, Cho SR. Retrograde jejuno gastric intussusception. *Rev Interam Radiol* 6: 21-24, 1981.
13. Shackman R. Jejunogastric intussusception. *Br J Surg* 27: 475-480, 1940.
14. Karlstrom L, Kelly KA. Ectopic jejunal pacemakers and gastric emptying after Roux gastrectomy: effect of intestinal pacing. *Surgery* 106: 867-871, 1989.
15. Navid AZ, Stephanie PH, Mark RR. Jejunogastric intussusception: a case report with the review of literature. *Emerg Radiol* 13: 265-267, 2007.
16. Mele CD, Porayko K. Jejunogastric intussusception, an indication for emergent endoscopy: case report. *Gastrointest Endosc* 57: 593-595, 2003.
17. Achyut JM, Ishwar JM, Jayantkumar BD, et al. Jejunogastric intussusception: case report and review of the literature. *Dig Endosc* 16: 88-90, 2004.
18. Lopez-Mut JV, Cubells M, Campos S, Miranda V, Rivera P. Je-

junogastric intussusception: a rare complication of gastric surgery. *Abdom Imaging* 23: 558-559, 1998.

© 2009 The Japanese Society of Internal Medicine
<http://www.naika.or.jp/imindex.html>

Role of carbon-11 choline PET/CT in the management of uterine carcinoma: initial experience

Keitaro Sofue · Ukihide Tateishi · Morio Sawada ·
Tetsuo Maeda · Takashi Terauchi · Daisuke Kano ·
Yasuaki Arai · Tomio Inoue · Kazuro Sugimura

Received: 12 September 2008 / Accepted: 27 November 2008 / Published online: 31 March 2009
© The Japanese Society of Nuclear Medicine 2009

Abstract

Purpose The present study was conducted to clarify the role of carbon-11 choline (^{11}C -choline) positron emission tomography (PET)/computed tomography (CT) in the management of uterine carcinoma.

Materials and methods Twenty-two patients who underwent ^{11}C -choline PET/CT and pelvic MRI were evaluated retrospectively. The images were reviewed by a board-certified radiologist and a nuclear medicine specialist who were unaware of any clinical information, and a consensus was reached. Diagnostic accuracy of PET/CT was evaluated for staging. The reference standard consisted of histological examination ($n = 17$) and follow-up conventional CT ($n = 5$). In five patients with cervical carcinoma, ^{11}C -choline PET/CT was performed before and after treatment that consisted of cisplatin infusion and subsequent radiotherapy.

Standardized uptake value (SUV) was compared with uni-dimensional and volumetric measurements that were made on magnetic resonance images (MRI) before and after treatment.

Results Based on PET/CT interpretations, the reviewers correctly classified T stage in 8 patients (47%), N stage in 21 patients (96%), M stage in 20 patients (91%), and TNM stage in 15 patients (88%). Tumor size, volume, and SUV decreased after treatment in five patients with cervical carcinoma. Using the Pearson correlation test, a significant correlation was found between the reduction rate of SUV and reduction rate of tumor volume.

Conclusions ^{11}C -choline PET/CT is an accurate means for the management of patients with uterine carcinoma. The combination of ^{11}C -choline PET/CT and MRI increases the accuracy of staging in patients with uterine carcinoma.

K. Sofue · Y. Arai
Division of Diagnostic Radiology,
National Cancer Center Hospital, Tokyo, Japan

U. Tateishi (✉) · T. Inoue
Department of Radiology, Yokohama City University
Graduate School of Medicine, 3-9 Fukuura, Kanazawa-ku,
Yokohama, Kanagawa 236-0004, Japan
e-mail: utateish@yokohama-cu.ac.jp

M. Sawada
Division of Gynecologic Oncology,
National Cancer Center Hospital, Tokyo, Japan

T. Maeda · K. Sugimura
Department of Radiology, Kobe University Graduate
School of Medicine, Hyogo, Japan

T. Terauchi · D. Kano
Division of Cancer Screening,
Research Center for Cancer Prevention and Screening,
National Cancer Center, Tokyo, Japan

Keywords PET/CT · Choline · Uterine

Introduction

Positron emission tomography (PET) with carbon-11 choline (^{11}C -choline) has been used to evaluate patients with a variety of malignant tumors [1–7]. Most studies have revealed that ^{11}C -choline PET is useful in the assessment of tumor stage [3–7]. More recently, PET studies using ^{11}C -choline as a tracer have been reported in patients with prostate cancer because of the minimal background activity in the pelvis due to the low level of excretion via the urinary tract which interferes with image evaluation [8]. ^{11}C -choline PET is also a feasible means of imaging uterine carcinomas [9], but the role of ^{11}C -choline PET scans in the preoperative staging of uterine carcinoma has not been clarified.

In the response evaluation criteria in solid tumors (RECIST), CT and magnetic resonance imaging (MRI) are considered the best currently available and the most useful tools for assessing the therapeutic effect on the target lesions, and the maximum diameter for the target lesions used as the reference to the objective tumor response [10]. However, the limited value of the RECIST criteria has been pointed out. PET with [^{18}F]-fluoro-2-deoxy-glucose (18F-FDG) has been used in the evaluation of patients with solid tumors, because the metabolic reduction precedes morphological changes [11]. Most studies on therapeutic response reveal that 18F-FDG-PET is superior in the assessment of therapeutic monitoring compared with conventional imaging [12–15]. PET has the potential to therapy monitoring in patients with cervical carcinoma. However, the exact role of ^{11}C -choline PET scan in the assessment of tumor response for cervical carcinomas has not been elucidated fully.

Positron emission tomography/computed tomography can improve tumor localization and staging accuracy because the anatomic and molecular information can be precisely co-registered [16]. The aim of the current study was to clarify the exact role of ^{11}C -choline PET/CT in the management of uterine carcinoma.

Materials and methods

Patients

We retrospectively reviewed the results of ^{11}C -choline PET/CT from January 2006 to December 2006 in patients with uterine carcinoma who either underwent radical hysterectomy and pelvic lymphadenectomy or were started on chemotherapy within a week. ^{11}C -choline PET/CT had been performed only for patients who had provided written informed consent to participate in the study and to a review of their records and images. A total of 22 patients with uterine carcinoma (cervical carcinoma, $n = 11$; corpus carcinoma, $n = 11$), which included preoperative studies for initial staging in all 22 patients, were enrolled into this study. In five patients with cervical carcinoma, both initial and follow-up examinations after chemotherapy in five patients were performed. The mean age was 51 years (range 31–73 years). The clinical records of all 22 patients were available for review. This study was conducted in accordance with the amended Helsinki declaration, and the protocol was approved by the Institutional Review Board.

PET/CT

Studies were performed with the LSO-based whole-body PET/CT scanner (Aquiduo; Toshiba). The CT component

of the scanner was the same as that of Aquillion 16, which has 16-rows detector. The PET component of the scanner has a transaxial field of view of 68.3 cm and an axial field of view of 16.2 cm without septa and rotating rod source. The scanner was used in 3D mode with image resolution of 4.0 mm in full width at half maximum (FWHM). Prior to the ^{11}C -choline PET/CT study, the patients fasted for at least 6 h. CT was performed from the head to the mid-thigh according to a standardized protocol with the following settings: axial 2.0-mm collimation \times 16 modes; 120 kVp; Auto-Exposure Control (SD10); and a 0.5-s tube rotation, a table speed of 11.0 mm/s. Patients maintained normal shallow respiration during the acquisition of CT scans. No iodinated contrast material was administered. ^{11}C -choline was synthesized with a commercial module described by Hara and co-workers [17]. Acquisition of emission scans from the head to the mid-thigh was started 5 min after intravenous administration of a mean ^{11}C -choline dose of 464 MBq (range, 409–560 MBq). Second emission scans of the pelvis were subsequently obtained starting 17 min of uptake time. The acquisition time for PET was 2 min per table position. Images were reconstructed with attenuation-corrected ordered-subset expectation maximization with 4 iterations and 14 subsets using emission scans and CT data.

Magnetic resonance imaging

MRI was performed within 2 weeks of ^{11}C -choline PET/CT, both before and after treatment. MRI was performed using a 1.5 T system (Signa Horizon LX, GE Medical Systems, Milwaukee). Pulse sequences comprised T1-weighted spin echo (SE) images (TR (repetition time)/TE (echo time): 500–600 ms/7–10 ms), T2-weighted fast spin echo (FSE) images (TR/TE: 3,750–4,400 ms/98–105 ms), as well as post-contrast T1-weighted SE images (TR/TE: 580–645 ms/6–10 ms) with fat suppression after injection of contrast material. All images were acquired in the transverse plane with a slice thickness of 5.0 mm, and a 1.0 mm intersection gap. The contrast material used was gadopentetate dimeglumine (Magnevist, Bayer Schering Pharma, Osaka, Japan) at a dose of 0.1 mmol/kg body weight. Pulse sequence parameters and slice orientation varied with the examined anatomic site. The images were reviewed and a consensus was reached by two board-certified radiologists who were unaware of any clinical or radiological information using multimodality computer platform.

Image interpretation

The images were reviewed by a board-certified radiologist and a nuclear medicine specialist who were unaware of any clinical information and a consensus was reached. PET,

CT, MRI, and co-registered PET/CT images were analyzed with dedicated software (e-soft; Siemens). PET, CT, and MRI were interpreted separately and co-registered PET/CT was read 6 months after the initial review. ^{11}C -choline uptake was considered abnormal when substantially greater than that of the surrounding normal tissue. A region of interest (ROI) of $1 \times 1\text{--}3 \times 3$ pixels was manually outlined within regions of increased ^{11}C -choline uptake and measured on each slice. For quantitative interpretations, the standardized uptake value (SUV) was determined according to the standard formula, with activity in the ROI recorded as Bq per ml/injected dose in Bq per weight (kg), but time decay correction for whole-body image acquisition was not performed. The maximum SUV (SUV max) was recorded using the maximum pixel activity within the ROI. We obtained 40% of maximum counts as the activity threshold. Both SUV max at a mean uptake time of 5 and 17 min were recorded as SUV₁ and SUV₂, respectively. The change in SUV was also calculated according to the formula: $\delta \text{ SUV (\%)} = (\text{SUV}_1 - \text{SUV}_2) / \text{SUV}_1 \times 100$. Uni-dimensional and volumetric measurements were conducted on MRI by the single radiologist. On the uni-dimensional measurement, tumor size was defined as the maximum diameter. On the volumetric measurement, tumor volume was calculated by a slice-by-slice evaluation. The area of the tumor was manually measured slice-by-slice on the transaxial post-contrast T1-weighted SE images with fat suppression, using manual segmentation with the multimodality computer platform. The measured area (cm²) per slice was multiplied by the factor 0.6 cm. The factor of 0.6 cm is based on the slice thickness of 5 mm and a distance factor of 1 mm. The volume of all measured slices containing tumor was summed up for total tumor volume.

Staging in cervical carcinoma

Tumor size by ^{11}C -choline PET/CT was determined based on the CT portion of the PET/CT. In tumors with unclear contour, tumor size was determined as the diameter of the cervix. T1 was considered when localized tumor with ^{11}C -choline uptake was depicted in the cervix. T2 was considered when tumor invaded the parametrium with ^{11}C -choline uptake for cervical carcinoma. T3 was considered when tumor with ^{11}C -choline uptake involved the serosa, adnexa, vagina, or peritoneal dissemination. Lymph nodes with abnormal uptake were recorded as positive for metastasis even when their short-axis diameter was less than 10 mm. N stage in six patients was confirmed by pathologic examination of specimens obtained by sampling of regional nodes. Nodal status of extraregional lymph nodes was confirmed in five patients by obvious regression in size of the lesions on follow-up MR examinations after

treatment. M stage was determined when paraaortic lymph node was involved or distant metastasis was found on contrast-enhanced CT during follow-up.

Staging in corpus carcinoma

Tumor size was also determined based on the CT portion of the PET/CT. In tumors with unclear contour, tumor size was determined as the diameter of the corpus. T1 was considered when localized tumor with ^{11}C -choline uptake was depicted in the corpus. T2 was considered when tumor involved the cervix with ^{11}C -choline uptake. T3 was considered when tumor with ^{11}C -choline uptake involved the serosa, adnexa, vagina, or peritoneal dissemination. Lymph nodes were classified similarly to those of cervical carcinoma. N stage was confirmed by pathologic examination of specimens obtained by sampling of regional nodes in all patients. M stage was determined when distant metastasis was found on contrast-enhanced CT during follow-up.

Treatment

In five patients with cervical carcinoma, treatment consisted of cisplatin infusion and subsequent radiotherapy. All but one of the patients, except one, were received chemotherapy consisting of cisplatin. One patient who had renal dysfunction did not receive chemotherapy. Radiotherapy comprised external beam radiotherapy (EBRT) 50 Gy and intra-cavitary radiotherapy (ICRT) 18–24 Gy. EBRT of the whole pelvis was performed and a total dose of 50 Gy was delivered at the rate of 2 Gy per fraction in 5 weeks. ICRT was performed and a total dose of 18–24 Gy was delivered at the rate of 8 Gy per fraction once a week. Four patients underwent chemotherapy with cisplatin (range 56–63 mg; mean 60.3 mg) once a week during EBRT. ^{11}C -choline PET/CT scans were performed before the start of treatment and after treatment.

Assessment of therapeutic response

The tumor size and volume from MRI after treatment were compared with those from the baseline study. The percentage of size reduction rate (%Size-RR) was calculated by the following formula; $[\text{Size (baseline)} - \text{Size (after treatment)}] / \text{Size (baseline)} \times 100$ (%). The percentage of volume reduction rate (%Volume-RR) was calculated by the following formula; $[\text{Volume (baseline)} - \text{Volume (after treatment)}] / \text{Volume (baseline)} \times 100$ (%).

Evaluation of metabolic response was accomplished by comparing the relative change in SUV, the percentage of SUV reduction rate (%SUV-RR). The SUV₁ and the SUV₂ from ^{11}C -choline PET/CT after treatment were compared with the baseline study. The percentage SUV₁ reduction

rate (%SUV₁-RR) was defined as the following formula; $[\text{SUV}_1 (\text{baseline}) - \text{SUV}_1 (\text{after treatment})] / \text{SUV}_1 (\text{baseline}) \times 100 (\%)$. The percentage SUV₂ reduction rate (%SUV₂-RR) was defined as the following formula; $[\text{SUV}_2 (\text{baseline}) - \text{SUV}_2 (\text{after treatment})] / \text{SUV}_2 (\text{baseline}) \times 100 (\%)$.

Statistical analysis

Each tumor was staged according to the TNM classification of the International Union Against Cancer (UICC) and the International Federation of Gynecology and Obstetrics (FIGO) Committee on Gynecologic Oncology [18, 19]. The mean follow-up period was 240 days (range 53–425 days). All variables were assessed on a patient-by-patient basis. Student's *t* test was used for paired comparisons of SUV. The McNemar test with Bonferroni's correction was used for paired comparisons between the results obtained by staging of ¹¹C-choline PET/CT. Therapeutic response was compared with imaging parameters using the Pearson correlation test. Correlation at a *P* value of less than 0.05 was considered to indicate a statistically significant difference. All data analysis was performed using software package SPSS 16.0J (SPSS, Chicago, IL, USA).

Results

Staging in cervical carcinoma

There were 11 cervical carcinomas (Table 1). Their histologic diagnoses were squamous cell carcinoma (*n* = 8), small cell carcinoma (*n* = 2), and adenosquamous carcinoma (*n* = 1). The tumor size of cervical carcinomas was 35 ± 14 mm. T stage was T1 in 2 patients (18%), T2 in 4 patients (36%), T3 in 3 patients (27%), and T4 in 1 patient (6%). The patient with T4 disease had rectal invasion microscopically. T stage was correctly classified by MRI alone in 6 patients (100%), by PET/CT alone in 3 patients (50%), and by PET/CT plus MRI in 6 patients (100%). Six (55%) of the 11 patients had N1 disease (Table 2). The accuracy of N staging was 73% by MRI alone, 91% by PET/CT alone, and 91% by PET/CT plus MRI. One patient had M1 disease with involvement of a paraaortic lymph node. The accuracy of M staging was 100% by PET/CT plus MRI as well as by PET/CT alone.

Staging in corpus carcinoma

The histologic diagnoses of 11 corpus carcinomas (Fig. 1) were endometrioid adenocarcinoma (*n* = 9), carcinosarcoma (*n* = 1), and serous adenocarcinoma (*n* = 1). The

Table 1 Demographic data of patients with cervical and corpus carcinomas

Parameter	Cervical carcinoma	Corpus carcinoma	Total
No. of patients	11	11	22
Age			
Mean ± SD	49 ± 12	53 ± 12	51 ± 12
Range	33–68	31–73	31–73
SUV ₁			
Mean ± SD	4.83 ± 1.87	5.92 ± 2.30	5.37 ± 2.12
Range	2.06–9.42	2.71–9.31	2.06–9.42
SUV ₂			
Mean ± SD	4.98 ± 1.97	5.82 ± 2.10	5.40 ± 2.04
Range	2.30–10.01	3.00–9.31	2.30–10.01
ΔSUV (%)			
Mean ± SD	-4.05 ± 14.01	0.40 ± 6.28	-1.82 ± 10.84
Range	-39.67–14.25	-10.70–14.00	-39.67–14.25
Final stage	IB (<i>n</i> = 2) IIB (<i>n</i> = 4) IIIB (<i>n</i> = 3) IVB (<i>n</i> = 1)	IA (<i>n</i> = 1) IB (<i>n</i> = 4) IIA (<i>n</i> = 1) IIIA (<i>n</i> = 2) IIIB (<i>n</i> = 1) IIIC (<i>n</i> = 2)	

SD standard deviation, SUV₁ SUV at a mean uptake time of 5 min, SUV₂ SUV at a mean uptake time of 18 min

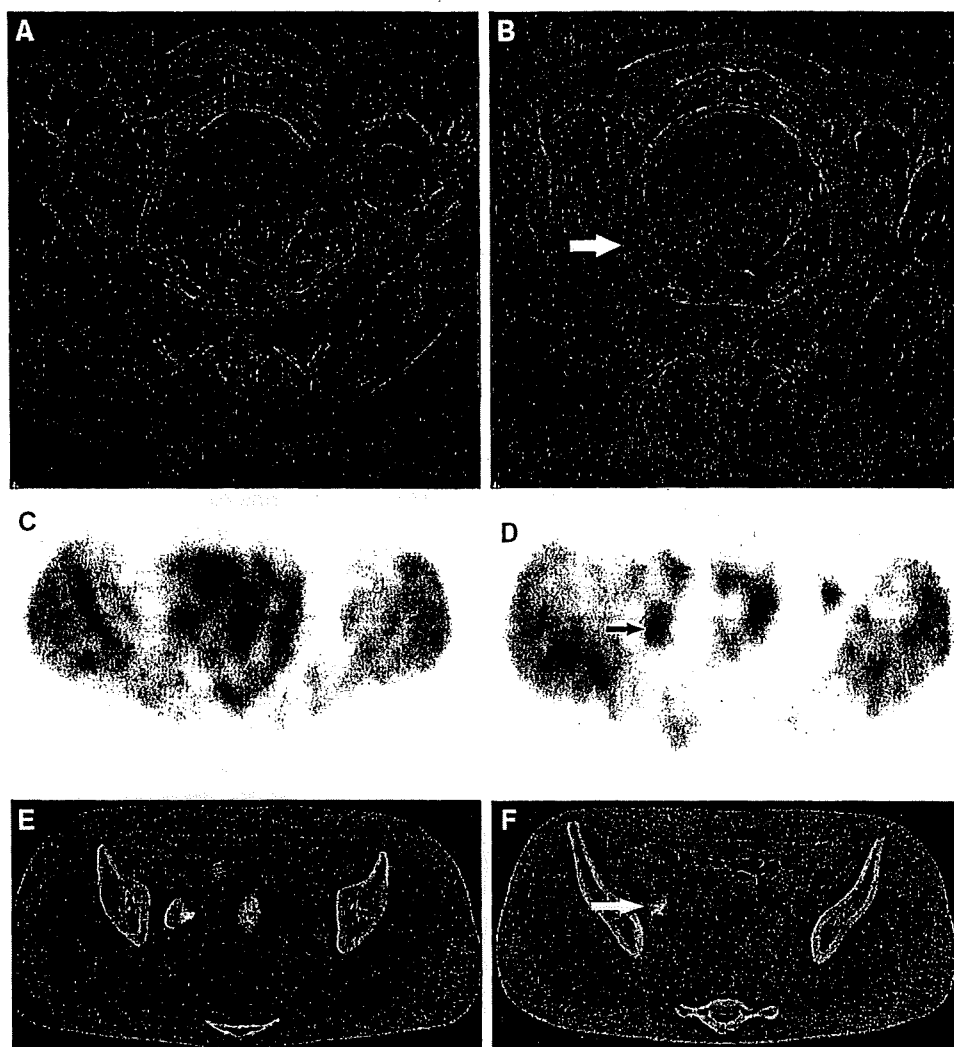
Table 2 Location of metastatic lymph nodes in all patients

Lymph node	No. of patients
Obturator	8 (36.3)
Common iliac	3 (13.6)
Paraaortic	2 (9.0)
External iliac	2 (9.0)
Internal iliac	2 (9.0)
Suprainguinal	1 (4.5)

The numbers in parentheses are percentages

histologic grades of the corpus carcinomas were Grade 1 (*n* = 6), Grade 2 (*n* = 3), and Grade 3 (*n* = 2). No significant differences in SUV₁ (*p* = 0.236) or SUV₂ (*P* = 0.348) of the primary lesion were found between cervical carcinoma and corpus carcinoma (Fig. 1). The ΔSUV in each type of tumor was similar at both primary sites (*P* = 0.347). The tumor size of the corpus carcinomas was 36 ± 21 mm. T stage was T1 in 5 patients (45%), T2 in 1 patient (6%), and T3 in 5 patients (45%). T stage was correctly classified by MRI alone in 9 patients (82%), by PET/CT alone in 5 patients (45%), and by PET/CT plus MRI in 10 patients (91%). One patient with corpus carcinoma who had developed a vaginal metastasis was understaged by MRI alone. After adding interpretation of PET/CT which showed discrete uptakes in the corpus and

Fig. 1 A 52-year-old woman with corpus carcinoma. **a, b** Transverse T2-weighted MR image (TR/TE_{eff}: 4,000 ms/100 ms) shows a primary tumor of the isthmus and enlargement of the right obturator lymph node (*arrow*). **c, d** Transverse ¹¹C-choline PET image reveals a hypermetabolic focus in the primary tumor and right obturator region (*arrow*). **e, f** Transverse ¹¹C-choline PET/CT image reveals a hypermetabolic focus in the primary tumor and right obturator lymph node (*arrow*). PET/CT findings were verified by histopathologic analysis



vagina, this patient was correctly diagnosed as having a vaginal metastasis. A patient with corpus carcinoma and peritoneal dissemination was understaged by MRI alone, whereas staging by PET/CT alone or PET/CT plus MRI was correct. Three (27%) of the 11 patients had N1 disease. The accuracy of N staging was 64% by MRI alone, 82% by PET/CT alone, and 100% by PET/CT plus MRI. All patients had M0 disease. The accuracy of M staging was 91% by PET/CT plus MRI and 82% by PET/CT alone. PET/CT alone overstaged two patients with corpus carcinoma as having distant metastasis, and their definitive diagnosis was vaginal metastasis and normal paraaortic lymph node, respectively. One patient with corpus carcinoma was overstaged by PET/CT plus MRI as having M1 disease.

Staging performance in uterine carcinomas

T stage (Table 3) was correctly classified by MRI alone in 15 patients (88%), by PET/CT alone in 8 patients (47%), and by PET/CT plus MRI in 16 patients (94%). MRI alone

or PET/CT plus MRI was superior to PET/CT alone in determining T stage ($P = 0.039$ or $P = 0.008$, respectively). PET/CT alone understaged four patients and overstaged five patients: The accuracy of N staging (Table 3) was 68% by MRI alone, 86% by PET/CT alone, and 96% by PET/CT plus MRI. PET/CT plus MRI was superior to MRI alone in assigning N stage ($P = 0.031$). MRI alone understaged four patients with subcentimetric lymph node and overstaged three patients with reactive lymph nodes. However, PET/CT alone understaged two patients with lymph node fewer than 10 mm in diameter and overstaged one patient with reactive lymph node. One patient with a lymph node was understaged by PET/CT plus MRI. The accuracy of M staging (Table 3) was 96% by PET/CT plus MRI and 91% by PET/CT alone. The overall stage (Table 3) was correctly diagnosed by PET/CT in 47%, and by PET/CT plus MRI in 88% ($P = 0.039$). PET/CT alone led to assignment of an incorrect TNM stage in nine patients due to misdiagnosis of T stage. Two patients were incorrectly diagnosed by PET/CT plus MRI.

Consequently, the misdiagnoses were in a patient with corpus carcinoma who had vaginal metastasis and a patient with a lymph node that measured fewer than 10 mm in diameter.

Table 3 Comparison of the diagnostic accuracy of staging by MRI, PET/CT, and combining PET/CT and MRI (PET/CT+MRI)

Diagnosis	MRI	PET/CT	PET/CT+MRI
T stage (n = 17)			
Correct	15 (88.2)*	8 (47.1)*†	16 (94.1)†
Overstaged	0	5 (29.4)	0
Understaged	2 (11.8)	4 (23.5)	1 (5.9)
N stage (n = 22)			
Correct	15 (68.2)†	19 (86.4)	21 (95.5)†
Overstaged	3 (13.6)	1 (4.5)	0
Understaged	4 (18.2)	2 (9.1)	1 (4.5)
M stage (n = 22)			
Correct	NA	20 (90.9)	21 (95.5)
Overstaged	NA	2 (9.0)	1 (4.5)
Understaged	NA	0	0
Overall stage (n = 17)			
Correct	NA	8 (47.1)†	15 (88.2)†
Overstaged	NA	5 (29.4)	1 (5.9)
Understaged	NA	4 (23.5)	1 (5.9)

The numbers in parentheses are percentages. The diagnostic accuracy of two modalities was compared by the McNemar test. Significant differences were found between two groups: * $P < 0.01$ and † $P < 0.05$

NA not applicable

Evaluation of therapeutic effect

Four (80%) of the five patients had IIb disease and one patient (20%) had IVa disease. One patient with IVa disease had bladder invasion and suffered from secondary bilateral hydronephrosis. Three patients (60%) had pelvic lymph node enlargement. Two of them were detected in bilateral obturator enlarged lymph nodes, and the other in right obturator enlarged lymph node. Distant metastases were not detected in any patients.

Baseline MRI showed that tumor size was 36.5 ± 8.7 mm. After treatment, the mean size was reduced to 21.8 ± 8.2 mm. Baseline MRI showed a tumor volume of 20.2 ± 12.6 cm³. After treatment, the mean volume was reduced to 12.2 ± 8.4 cm³ (Fig. 2). The %Size-RR was $40.7 \pm 12.8\%$ and the %Volume-RR was $56.5 \pm 10.3\%$ (Table 4).

All five patients had abnormal ¹¹C-choline uptake of the primary lesion on initial PET/CT. SUV₁ and SUV₂ after chemoradiotherapy decreased compared with that before chemoradiotherapy. Baseline PET/CT showed a mean SUV₁ of 5.3 ± 2.4 , and a mean SUV₂ of 5.2 ± 2.7 . After treatment, the SUV₁ decreased to 2.6 ± 1.2 , and the SUV₂ decreased to 2.0 ± 1.0 (Fig. 2). The %SUV₁-RR was $48.0 \pm 20.0\%$ and %SUV₂-RR was $60.3 \pm 14.4\%$ (Table 5).

The correlation between %SUV₁-RR and %Size-RR was not significant ($r = 0.698$, $P = 0.19$), while there was a significant correlation between %SUV₁-RR and %Volume-RR ($r = 0.892$, $P = 0.042$). Indeed, there was

Fig. 2 A 60-year-old woman with cervical carcinoma: Transverse T2-weighted MR image on the baseline study (a) shows an isointense tumor of uterine cervix. The tumor size and volume are 32.6 mm and 12.59 cm³, respectively. After treatment (b), the tumor is reduced in size. The tumor size and volume are 16.4 mm and 5.63 cm³, respectively. Transverse ¹¹C-choline PET/CT image on the baseline study (c) shows an increased metabolic uptake in primary tumor. After treatment (d), metabolic uptake in the primary tumor decreases. The SUV₁ and SUV₂ decrease from 4.61 and 4.61 to 2.10 and 1.90, respectively

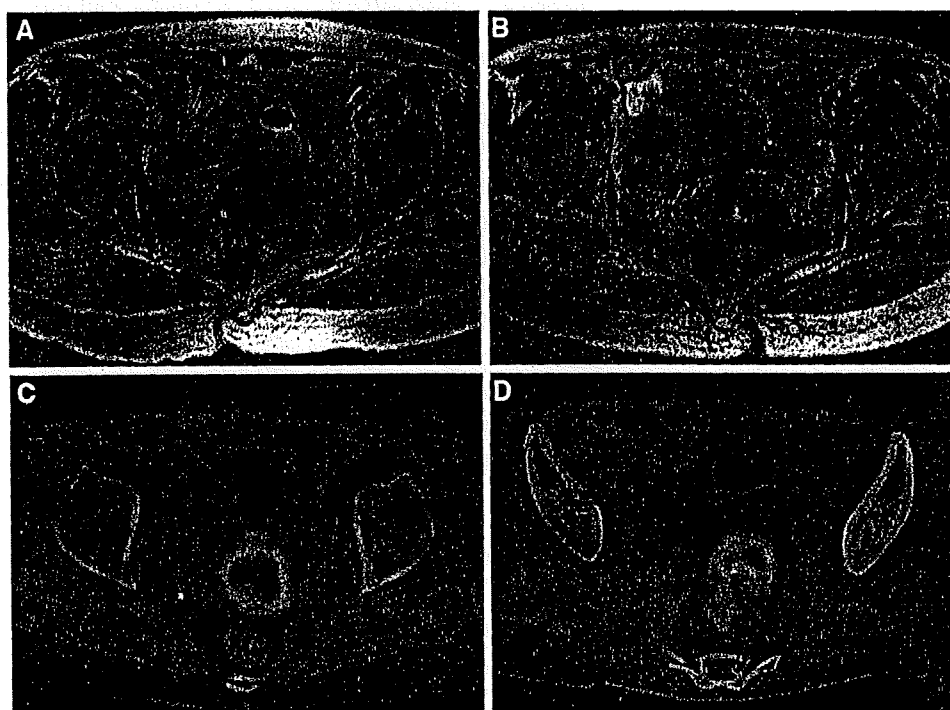


Table 4 Clinical characteristics in five patients with cervical carcinoma

Pt	Age	Chief complaint	Histology	Chemo		RT		Recurrence time (months)	Treatment after recurrence	Follow-up time (months)
				Dose (mg)	Cycle	EBRT	ICRT			
1	60	Vaginal bleeding	Squamous	56	1	50 Gy/25fr	18 Gy/3fr	3	Chemo	13
2	68	Vaginal bleeding	Squamous	0	0	50 Gy/25fr	18 Gy/3fr	8	None	14
3	55	Vaginal bleeding	Squamous	56	5	50 Gy/25fr	18 Gy/3fr	7	RT	16
4	35	Vaginal bleeding	Squamous	62.2	4	50 Gy/25fr	24 Gy/4fr	None	None	15
5	57	Vaginal bleeding	Squamous	63.4	4	50 Gy/25fr	18 Gy/3fr	None	None	13

Pt patient, Chemo chemotherapy, RT radiotherapy, EBRT extra body radiotherapy, ICRT intra cervical radiotherapy, squamous squamous cell carcinoma, fr fraction

Table 5 Assessment of MRI and ^{11}C -choline PET results in five patients with cervical carcinoma

Pt	MRI							
	Diameter (mm)				Volume (cm^3)			
	Baseline	After	δ	RR (%)	Baseline	After	δ	RR (%)
1	32.6	16.4	16.2	49.7	12.59	5.63	6.96	55.3
2	40.7	28.4	12.3	30.2	31.64	14.78	16.86	53.3
3	45.5	32.7	12.8	28.1	21.37	8.57	12.81	59.9
4	23.3	14.5	8.8	37.8	2.99	1.71	1.28	42.9
5	40.6	17.1	23.5	57.9	32.27	9.27	23.01	71.3

Pt	^{11}C -choline PET							
	SUV ₁				SUV ₂			
	Baseline	After	δ	RR (%)	Baseline	After	δ	RR (%)
1	9.42	4.29	5.13	54.5	10.01	3.6	6.41	64
2	3.57	2.6	0.97	27.2	3.57	1.51	2.06	57.7
3	4.61	2.1	2.51	54.4	4.61	1.9	2.71	58.8
4	4.28	3.04	1.24	29	3.67	2.19	1.48	40.3
5	4.4	1.1	3.3	75	4.1	0.8	3.3	80.5

Pt patient, Baseline baseline study, After study after treatment, δ difference between baseline study and study after treatment, RR reduction rate

no significant correlation between %SUV₂-RR and %Size-RR ($r = 0.660$, $P = 0.226$), while there was a significant correlation between %SUV₂-RR and %Volume-RR ($r = 0.956$, $P = 0.011$). During a mean follow-up time of 14.2 ± 1.0 months, two patients developed disease recurrence. One patient had a local recurrence three months after the treatment, and received additional chemotherapy using cisplatin and paclitaxel. The other patient developed metastasis of a paraaortic lymph node seven months after the treatment, and received radiotherapy of the abdomen. No patients died before disease recurrence.

Discussion

The results of the present study show that ^{11}C -choline PET/CT contributes to accurate staging in patients with uterine

carcinoma. Specifically, the combination of ^{11}C -choline PET/CT and MRI has potential implications for determining T and N stage at the preoperative evaluation. The results of the present study also indicate that ^{11}C -choline PET/CT may be feasible as a method of evaluating the therapeutic response after chemoradiotherapy in patients with cervical carcinoma.

Clinically, requirements for an acceptable method of preoperative staging of uterine carcinoma are that it allows determination of appropriate indications for surgery. Measured by this criterion, MRI has long been recognized as the most accurate modality, with high sensitivity [20, 21]. However, the limitation in MR evaluation for preoperative staging of uterine carcinoma is low specificity for N staging. In our study the interpretation of N staging by combining ^{11}C -choline PET/CT and MRI yielded an accuracy of 96%. The results of the present study suggest